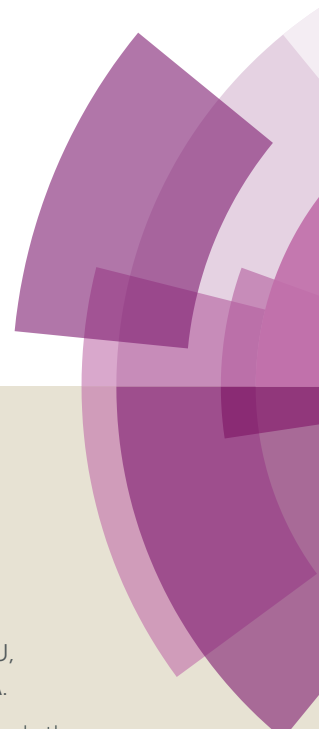


# Journal of Materials Chemistry C

Accepted Manuscript



This article can be cited before page numbers have been issued, to do this please use: Y. Xiang, Z. ZHU, D. Xie, S. Gong, K. Wu, G. Xie, C. Lee and C. Yang, *J. Mater. Chem. C*, 2018, DOI: 10.1039/C8TC01656A.



This is an Accepted Manuscript, which has been through the Royal Society of Chemistry peer review process and has been accepted for publication.

Accepted Manuscripts are published online shortly after acceptance, before technical editing, formatting and proof reading. Using this free service, authors can make their results available to the community, in citable form, before we publish the edited article. We will replace this Accepted Manuscript with the edited and formatted Advance Article as soon as it is available.

You can find more information about Accepted Manuscripts in the [author guidelines](#).

Please note that technical editing may introduce minor changes to the text and/or graphics, which may alter content. The journal's standard [Terms & Conditions](#) and the ethical guidelines, outlined in our [author and reviewer resource centre](#), still apply. In no event shall the Royal Society of Chemistry be held responsible for any errors or omissions in this Accepted Manuscript or any consequences arising from the use of any information it contains.

## Revealing new potential of an indandione unit for constructing efficient yellow thermally activated delayed fluorescence emitters with short emissive lifetimes

Received 00th January 20xx,  
Accepted 00th January 20xx

DOI: 10.1039/x0xx00000x

www.rsc.org/

Yepeng Xiang,<sup>a,b</sup> Ze-Lin Zhu,<sup>c,d</sup> Dongjun Xie,<sup>a</sup> Shaolong Gong,<sup>\*a</sup> Kailong Wu,<sup>a</sup> Guohua Xie,<sup>a</sup> Chun-Sing Lee,<sup>\*c,d</sup> Chuluo Yang<sup>\*a,b</sup>

Simultaneously accomplishing a high efficiency and a slow efficiency roll-off at the practical luminance levels remains challenging for thermally activated delayed fluorescence (TADF) organic light-emitting diodes (OLEDs). In this study, for the first time, we reveal new potential of indandione unit featuring double carbonyl moieties, which is widely used in organic solar cells, as an electron-accepting core for constructing efficient TADF emitters. As a proof of concept, two TADF emitters, 5PXZ-PIDO and 5,6PXZ-PIDO, are developed by connecting an indandione (IDO) core with electron-donating phenoxazine (PXZ) units *via* the phenylene  $\pi$ -bridges. Impressively, both emitters exhibit distinct TADF nature with short DF lifetimes of  $\sim 2 \mu\text{s}$ , and display relatively high photoluminescence quantum yields ( $\Phi_{\text{PLS}}$ ) of over 70%. More importantly, a yellow OLED based on 5,6PXZ-PIDO achieves a high EQE of 14.2% and an ultra-slow efficiency roll-off of 16.0% at a practical luminance of  $1000 \text{ cd m}^{-2}$ , which is outstanding among previously reported carbonyl-based TADF emitters. This finding unlocks the huge potential of indandione-based molecules as TADF emitters for high-performance OLEDs.

### Introduction

Due to the unique capability of effectively harvesting triplet excitons in organic light-emitting diodes (OLEDs), thermally activated delayed fluorescence (TADF) emitters have attracted considerable attentions in academic and industrial communities during the past few years. Since the pioneering discovery of introducing TADF emitters into OLEDs by Adachi and co-authors, much endeavor has been devoted to extending molecular diversity of TADF emitters and enhancing their device performance.<sup>1-6</sup> Although blue TADF emitters have been the most important concern, other color TADF emitters including yellow emitters are also necessary for developing efficient white OLEDs, hyperfluorescence OLEDs and so on. So far, considerable progresses have been achieved in multi-color TADF OLEDs with external quantum efficiencies (EQEs) of over 20%.<sup>7-18</sup> However, most of TADF OLEDs generally suffer from drastic efficiency roll-offs at a practical luminance because of the relatively long DF lifetimes of TADF emitters. In this sense,

simultaneously accomplishing a high efficiency and a slow efficiency roll-off at a practical luminance levels remains challenging for TADF OLEDs.<sup>19-21</sup> New efficient multi-color TADF emitters with reduced DF lifetimes of less than  $5 \mu\text{s}$  are therefore highly required to address this issue.<sup>7-12,17</sup>

A common way to reduce DF lifetimes of TADF emitters is to minimize energy gap ( $\Delta E_{\text{ST}}$ ) between the lowest singlet and triplet states through increasing twisting angles between electron donor and acceptor units, and lowering overlapping of their frontier molecular orbitals. However, this approach normally leads to low oscillator strength ( $f$ ) of TADF emitters, and thus sacrifices their photoluminescence quantum yields ( $\Phi_{\text{PLS}}$ ). Recently several groups developed some TADF emitters with reduced DF lifetimes by adopting multi-dipolar transition structure in molecular design.<sup>22-24</sup> For example, Xu *et al.* reported a multi-dipolar TADF emitter featuring phosphine oxide units, and the corresponding device exhibited blue emission and reduced efficiency roll-offs at a practical luminance.<sup>24</sup> This may provide a feasible strategy of reducing DF lifetimes of TADF emitters without sacrificing their  $\Phi_{\text{PLS}}$ .

Carbonyl-based moieties are widely used as electron acceptors for constructing organic functional materials for OLEDs and organic solar cells (OSCs).<sup>25-28</sup> Among them, an indandione (IDO) unit containing double carbonyl moieties has been established to be an effective electron acceptor, in virtue of its strong electron-withdrawing ability and multiple modification sites. However, the introduction of IDO-based emitters into OLEDs has not been explored. In consideration of intrinsic double accepting structure in the IDO unit, we, herein,

<sup>a</sup>Hubei Key Lab on Organic and Polymeric Optoelectronic Materials, Department of Chemistry, Wuhan University, Wuhan, 430072, P. R. China.

\*E-mail: slgong@whu.edu.cn, clyang@whu.edu.cn.

<sup>b</sup>Shenzhen Key Laboratory of Polymer Science and Technology, College of Materials Science and Engineering, Shenzhen University, Shenzhen 518060, P. R. China.

<sup>c</sup>Center of Super-Diamond and Advanced Films (COSDAF) and Department of Chemistry, City University of Hong Kong, Hong Kong SAR, P. R. China.

<sup>d</sup>City University of Hong Kong Shenzhen Research Institute, Shenzhen, Guangdong, P. R. China.

\*E-mail: apclee@cityu.edu.hk.

† Electronic Supplementary Information (ESI) available

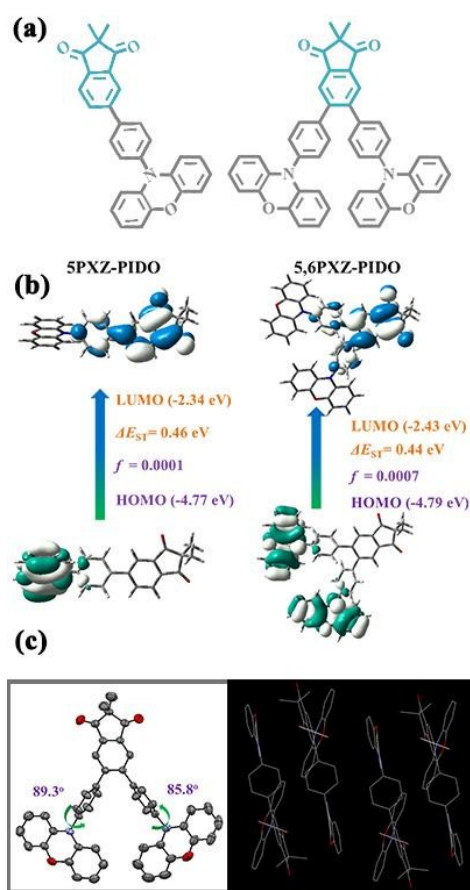


**Fig. 1** (a) The chemical structures of 5PXZ-PIDO and 5,6PXZ-PIDO. (b) The FMO, energy levels, oscillator strength ( $f$ ) of 5PXZ-PIDO and 5,6PXZ-PIDO [upon B3LYP level and 6-31G(d) set for DFT; upon LC- $\omega$ \*PBE level and 6-31G(d) set for TD-DFT]. (c) ORTEP diagram molecular packing diagram of 5,6PXZ-PIDO with hydrogen atoms omitted.

developed two TADF emitters, namely, 5PXZ-PIDO and 5,6PXZ-PIDO, by incorporating electron-donating phenoxazine (PXZ) units into an IDO core *via* the phenylene  $\pi$ -bridges (**Scheme 1**). Methyl groups are introduced into the active methylene group of IDO unit to avoid side reactions and suppress intermolecular  $\pi$ - $\pi$  interaction. Remarkably, both emitters display distinct TADF features and relatively short DF lifetimes of  $\sim 2$   $\mu$ s, and exhibit relatively high  $\Phi_{\text{PLS}}$  of over 70%. To the best of our knowledge, this is the first report on IDO-based compounds with TADF feature. As a result, 5,6PXZ-PIDO successfully achieves an intense yellow emission with a high EQE of 16.9%. Moreover, its EQE remains as high as 14.2%, corresponding to an ultra-slow efficiency roll-off of 16.0%, at the practical luminance of 1000 cd m $^{-2}$ , which is prominent among previously reported carbonyl-based TADF emitters.<sup>8,20,29-35</sup>

## Experimental section

The corresponding halogen precursors of PIDO-Br and PIDO-2Cl were prepared according to literature precedence (**Scheme S1**).<sup>36</sup>

**5-(4-(10H-phenoxazin-10-yl)phenyl)-2,2-dimethyl-1H-indene-1,3(2H)-dione (5PXZ-PIDO):** To a mixture of 10-(4-(4,4,5,5-

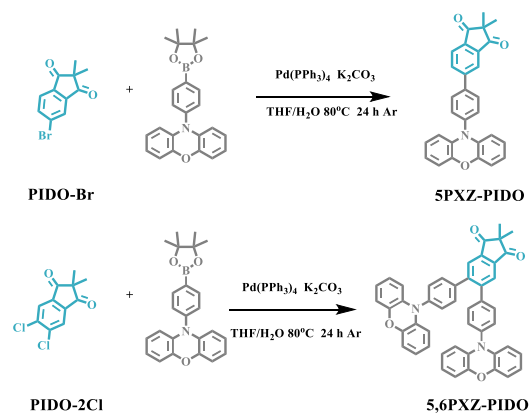
tetramethyl-1,3,2-dioxaborolan-2-yl)phenyl)-10H-phenoxazine (424 mg, 1.1 mmol), 5-bromo-2,2-dimethyl-1H-indene-1,3(2H)-dione (PIDO-Br) (252 mg, 1 mmol), potassium carbonate (276 mg, 2 mmol) and Pd(PPh $_3$ ) $_4$  (10 mg, 0.01 mmol) was added 20 mL of degassed tetrahydrofuran and 10 mL of degassed water. After stirring at 80  $^{\circ}$ C under an argon atmosphere for 24 h, the mixture was cooled down to room temperature and extracted with 3  $\times$  40 mL of dichloromethane. The collected organic phase was washed with brine and dried with anhydrous Na $_2$ SO $_4$ . After removal of the solvent, the residue was purified by column chromatography on silica gel (eluent: petroleum/dichloromethane = 1:1, v/v) to afford the product as red powder (300 mg, yield: 70%).  $^1$ H NMR (400 MHz, CDCl $_3$  + TMS, 25  $^{\circ}$ C)  $\delta$  [ppm]: 8.24 (d,  $J$  = 1.5 Hz, 1H), 8.15 (dd,  $J$  = 8.0, 1.6 Hz, 1H), 8.10 (d,  $J$  = 8.0 Hz, 1H), 7.90 (d,  $J$  = 8.4 Hz, 2H), 7.51 (d,  $J$  = 8.4 Hz, 2H), 6.77-6.54 (m, 6H), 6.00 (d,  $J$  = 7.6 Hz, 2H), 1.36 (s, 6H).  $^{13}$ C NMR (100 MHz, CDCl $_3$ , 25  $^{\circ}$ C)  $\delta$  [ppm]: 204.53, 204.06, 147.94, 143.96, 141.20, 139.97, 139.03, 134.84, 134.05, 131.80, 130.17, 124.35, 123.30, 121.85, 121.65, 115.63, 113.24, 50.40, 20.40. MS (HRMS): Anal. Calcd for C $_{29}$ H $_{22}$ NO $_3$  $^+$  432.15942 [M+H] $^+$ . found: 432.15927 [M+H] $^+$ .

**5,6-Bis(4-(10H-phenoxazin-10-yl)phenyl)-2,2-dimethyl-1H-indene-1,3(2H)-dione (5,6PXZ-PIDO):** Prepared according to the same procedure as 5PXZ-PIDO but using PIDO-2Cl. Yield: 73%.  $^1$ H NMR (400 MHz, CDCl $_3$  + TMS, 25  $^{\circ}$ C)  $\delta$  [ppm]: 8.17 (s, 2H), 7.43 (d,  $J$  = 8.4 Hz, 4H), 7.31 (d,  $J$  = 8.4 Hz, 4H), 6.77-6.41 (m, 12H), 5.85 (d,  $J$  = 7.5 Hz, 4H), 1.40 (s, 6H).  $^{13}$ C NMR (100 MHz, CDCl $_3$ )  $\delta$  [ppm]: 204.12, 148.02, 143.86, 139.64, 138.96, 133.97, 132.39, 130.95, 125.29, 123.45, 121.59, 115.55, 112.97, 50.48, 20.44. MS (HRMS): Anal. Calcd for C $_{47}$ H $_{32}$ N $_2$ O $_4$  $^+$  688.23566 [M] $^+$ . found: 688.23566 [M] $^+$ .

## Results and discussion

Frontier molecular orbitals (FMOs) and the excited states of both molecules were predicted by density functional theory (DFT) and time-dependent DFT (TD-DFT) calculations. **Fig. 1b** depicted the HOMO and LUMO distributions of both molecules. Apparently, both molecules exhibited well-separated HOMO and LUMO distributions, accompanied with small overlaps on the phenylene bridges. Such distributions imparted both molecules with small  $\Delta E_{\text{ST}}$ s of around 0.45 eV, indicating that RISC process based on  $T_1 \rightarrow S_1$  may occur in these molecules. In comparison with 5PXZ-PIDO with a single-dipolar structure, 5,6PXZ-PIDO possessed the higher oscillator strength ( $f$ ) originating from its double-dipolar transition structure, suggesting that 5,6PXZ-PIDO may perform as the better emitter.<sup>37,38</sup>

The synthetic routes for two IDO-cored compounds were outlined in **Scheme 1**. Both compounds were produced by Pd-catalyzed C-C cross-coupling reaction of 10-(4-(4,4,5,5-tetramethyl-1,3,2-dioxaborolan-2-yl)phenyl)-10H-phenoxazine with the corresponding halogen precursors in high yields, respectively. 5PXZ-PIDO and 5,6PXZ-PIDO were purified by recrystallization and further gradient sublimation, and their structures were verified by  $^1$ H NMR,  $^{13}$ C NMR and high-



Scheme 1 Synthesis of 5PXZ-PIDO and 5,6PXZ-PIDO

resolution mass spectrometry (Fig. S1-S10). Furthermore, the molecular structure of 5,6PXZ-PIDO was identified by the single-crystal X-ray crystallographic analysis. As shown in Fig. 1c, 5,6PXZ-PIDO preferred a quasi-symmetry orientation with the large torsion angles of 89.3° and 85.8° between the PXZ unit and the adjacent phenylene bridge, which is consistent with the DFT results.

Both compounds exhibited relatively high decomposition temperatures ( $T_d$ , corresponding to 5% weight loss) over 400 °C. The DSC traces revealed their glass transition temperatures ( $T_g$ s) of 134 °C for 5PXZ-PIDO and 164 °C for 5,6PXZ-PIDO, respectively (Fig. 2a). These results clearly established the high thermal stability of both compounds, which could benefit device stability under long-term operation condition.<sup>15,39</sup> The electrochemical properties of the two compounds were studied by cyclic voltammetry (CV) experiments. According to the half-wave potentials of two compounds in CV curves (Fig. 2b), the HOMO/LUMO levels of 5PXZ-PIDO and 5,6PXZ-PIDO were established to be -5.10/-2.80 eV and -5.08/-2.81 eV, respectively (Table 1). The favorable HOMO/LUMO levels of both compounds could benefit charge injection between the emitting layer and the adjacent charge-transporting layers in OLEDs.

As presented in Fig. 3, 5PXZ-PIDO and 5,6PXZ-PIDO exhibited two types of absorption bands simultaneously in toluene: strong absorption bands in the high-energy region (280-350 nm), mainly attributed to locally excited (LE) transitions of PXZ and/or IDO units (Fig. S11), and tailed absorption bands in the region of 360-450 nm, assigned to intramolecular charge transfer (ICT) transition from PXZ to IDO units. Moreover, both emitters displayed structureless emission with main peaks at 564 and 573 nm for 5PXZ-PIDO and 5,6PXZ-PIDO, respectively, in toluene. Under degassed condition, both emitters exhibited double exponential decays containing prompt and delayed fluorescence components. The emissive characteristics of both emitters in film state were also investigated in 4,4'-di(9H-carbazol-9-yl)-1,1'-biphenyl (CBP) host, which is a widely used host in OLEDs because of its bipolar charge-transporting ability and relatively high triplet energy. Both compounds in CBP (1.5 wt.%) host exhibited broad emission bands with the emission peaks at 535 and 544 nm for 5PXZ-PIDO and 5,6PXZ-PIDO, respectively. As shown in

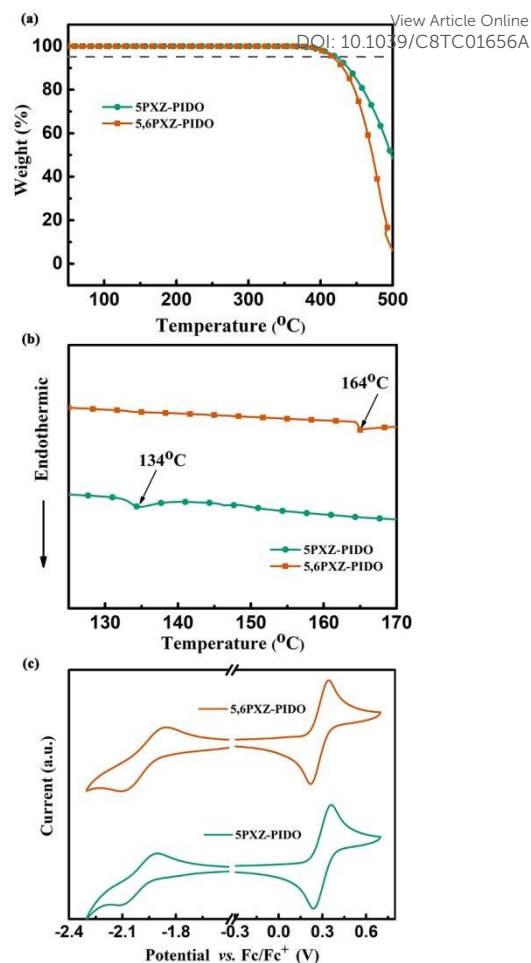


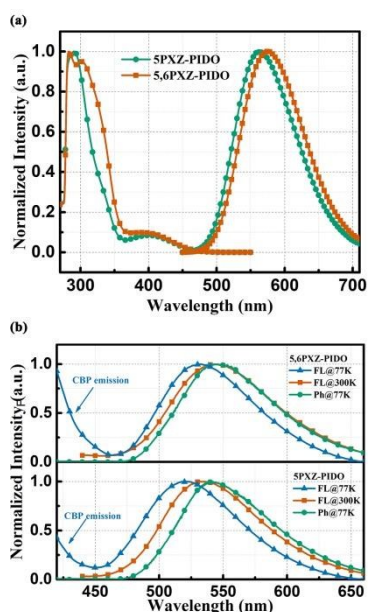
Fig. 2 (a) TGA curves of 5PXZ-PIDO and 5,6PXZ-PIDO. (b) DSC curves of 5PXZ-PIDO and 5,6PXZ-PIDO. (c) Oxidation and reduction behaviors of 5PXZ-PIDO and 5,6PXZ-PIDO.

Fig. 3b, 5PXZ-PIDO exhibited the same FWHM (full-width at half-maximum) of 85 nm in its Ph. and low-temperature fluorescence spectra. The same case was observed for 5,6PXZ-PIDO (a FWHM of ~ 87 nm) in its Ph. and low-temperature fluorescence spectra. At room temperature, the more active vibrations and rotations in both emitters widened their FL spectra. According to the onsets of the corresponding fluorescence and phosphorescence spectra, the singlet and triplet state energy of both emitters were estimated to be 2.61/2.57 eV and 2.58/2.56 eV, respectively. As a result, the  $\Delta E_{\text{ST}}$ s of both emitters in CBP host were calculated to be 0.04 eV for 5PXZ-PIDO and 0.02 eV for 5,6PXZ-PIDO. These results are basically consistent with the outcomes of both emitters doped into PMMA (1.5 wt.%) films (Fig. S12), clearly revealing that these emissive characteristics originate from the emitters. The small  $\Delta E_{\text{ST}}$ s of both compounds suggest that RISC process based on  $T_1 \rightarrow S_1$  may easily occur in both emitters. To figure out emissive nature of both emitters, transient PL spectra of 5PXZ-PIDO and 5,6PXZ-PIDO in CBP host (1.5 wt.%) were studied. Apparently, both emitters displayed second-order exponential decay with prompt (16.0 ns for 5PXZ-PIDO and 15.0 ns for 5,6PXZ-PIDO) and delayed (2.37  $\mu$ s for 5PXZ-PIDO and 1.98  $\mu$ s for 5,6PXZ-PIDO) components in CBP host. Compared with 5PXZ-PIDO, 5,6PXZ-PIDO with a double-dipolar

**Table 1** Thermal, electrochemical and photophysical properties of 5PXZ-PIDO and 5,6PXZ-PIDO

compounds	$\lambda_{\text{abs}}^a/\lambda_{\text{PL}}^b$ [nm]	HOMO <sup>c</sup> /LUMO <sup>c</sup> [eV]	$T_g^d/T_d^e$ [°C]	$\Delta E_{\text{ST}}^f/\Delta E_{\text{ST}}^g$ [eV]	$\tau_p^h$ [ns]	$\tau_d^h$ [μs]	$\Phi^i$ [%]	$\Phi_p/\Phi_d^j$ [%]	$k_f/k_{\text{ISC}}^k$ [10 <sup>7</sup> s <sup>-1</sup> ]	$k_{\text{RISC}}^k$ [10 <sup>5</sup> s <sup>-1</sup> ]
5PXZ-PIDO	291/535	-5.10/-2.80	134/421	0.04/0.11	16	2.37	72	48/24	6.25/3.25	4.06
5,6PXZ-PIDO	283/544	-5.08/-2.81	164/417	0.02/0.06	15	1.98	76	47/29	6.67/3.53	5.89

<sup>a</sup> Measured in toluene solution (10<sup>-5</sup> M) at room temperature. <sup>b</sup> Measured in doped CBP films (1.5 wt.%) at room temperature. <sup>c</sup> Obtained from cyclic voltammograms in CH<sub>2</sub>Cl<sub>2</sub> solution. <sup>d</sup> Obtained from DSC measurements. <sup>e</sup> Obtained from TGA measurements ( $T_d$ , corresponding to 5% weight loss). <sup>f</sup> Calculated from the onset of the fluorescence (room temperature) and phosphorescence spectra (77 K) of the two emitters doped in CBP films (1.5 wt.%). <sup>g</sup> Calculated from the onset of the fluorescence (77 K) and phosphorescence spectra (77 K) of the two emitters doped in CBP films (1.5 wt.%). <sup>h</sup> The prompt and delayed fluorescence lifetimes of emitters doped into CBP films (1.5 wt.%) at room temperature. <sup>i</sup> The total PLQYs of emitters doped into CBP films (1.5 wt.%) under oxygen-free condition at room temperature. <sup>j</sup> The prompt and delayed fluorescence PLQY under oxygen-free condition. <sup>k</sup> The rate constants of radiative, ISC and RISC process in CBP host.



**Fig. 3** (a) The UV-Vis absorption and fluorescence curves of 5PXZ-PIDO and 5,6PXZ-PIDO in toluene (10<sup>-5</sup> M), and (b) low temperature fluorescence (77 K), room temperature fluorescence (300 K) and phosphorescence (77 K) spectra of the two compounds doped into CBP films (1.5 wt.%).

transition structure possessed smaller  $\Delta E_{\text{ST}}$  and shorter delay lifetime, consistent with the previous work.<sup>24,38</sup> Moreover, the intensity of the delayed component for both emitters gradually increased with increasing temperature from 100 to 300 K, clearly establishing distinct TADF nature of both emitters. The  $\Phi_{\text{PLS}}$  of 5PXZ-PIDO and 5,6PXZ-PIDO in CBP host were estimated to be 72% and 76%, respectively, at room temperature. In comparison with 5PXZ-PIDO, the slightly enhanced  $\Phi_{\text{PL}}$  of 5,6PXZ-PIDO could be ascribed to the higher oscillator strength ( $f$ ) originating from its double-dipolar transition structure. To further understand the ISC and RISC processes for both emitters in CBP host, the rate constants of ISC and RISC process for both emitters were estimated to be  $3.25 \times 10^7/4.06 \times 10^5$  s<sup>-1</sup> and  $3.53 \times 10^7/5.89 \times 10^5$  s<sup>-1</sup> (Table 1). Apparently, both emitters exhibited almost the same  $k_{\text{ISC}}$ ; while, the smaller  $\Delta E_{\text{ST}}$  endowed 5,6PXZ-PIDO with the larger  $k_{\text{RISC}}$ . Furthermore, the radiative rate constant  $k_f$  of 5PXZ-PIDO and 5,6PXZ-PIDO in CBP films were estimated to be  $6.25 \times 10^7$  s<sup>-1</sup> and  $6.67 \times 10^7$  s<sup>-1</sup>, respectively, which match well with the DFT results that the  $f$  of the 5,6PXZ-PIDO was larger than that of

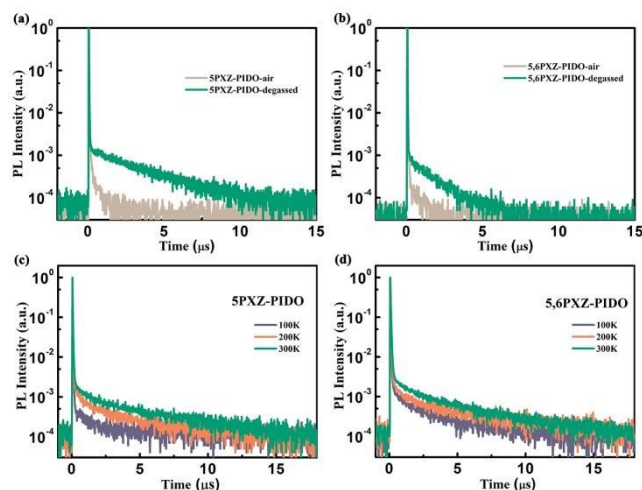


**Fig. 4** The transient photoluminescence decay spectra of (a) 5PXZ-PIDO and (b) 5,6PXZ-PIDO in toluene (10<sup>-5</sup> M) under aerated and degassed condition. The transient photoluminescence decay spectra of (c) 5PXZ-PIDO and (d) 5,6PXZ-PIDO doped into CBP films (1.5 wt.%) at various temperatures.

the 5PXZ-PIDO.

Inspired by the excellent features of high  $\Phi_{\text{PLS}}$ , obvious TADF feature and short delayed lifetimes, 5PXZ-PIDO and 5,6PXZ-PIDO were employed as emitters in multi-layer OLEDs with an architecture of ITO/TAPC (30 nm)/TCTA (5 nm)/CBP: TADF emitters (1.5 wt.%, 20 nm)/TmPyPB (65 nm)/LiF (1 nm)/Al (120 nm) (Fig. 5a). Wherein, TAPC and TmPyPB acted as the hole- and electron-transporting layer, respectively; TCTA was inserted between TAPC and the emitting layer to facilitate hole injection/transport and suppress the detrimental quenching process between the excess holes and the emissive excitons; 5PXZ-PIDO and 5,6PXZ-PIDO were doped into CBP host with an optimal doping concentration of 1.5 wt.% (Table S4) as the emission layer for devices A and B, respectively. Devices A and B displayed yellow light and favorable Commission International de l'Éclairage coordinates of (0.39, 0.54) and (0.42, 0.53), respectively. Furthermore, the EL spectra of both devices remained the same under difference current density (Fig. S13), indicative of the balanced charge carrier injection and transportation in the emission layer for both devices. Both devices exhibited similar current density-voltage ( $J$ - $V$ ) characteristics with the almost same turn-on voltages (c.a. 3.5 eV), which can be attributed to the same OLED architecture and the similar HOMO/LUMO levels of both emitters. As shown in Fig. 5d, device A based on 5PXZ-PIDO exhibited a

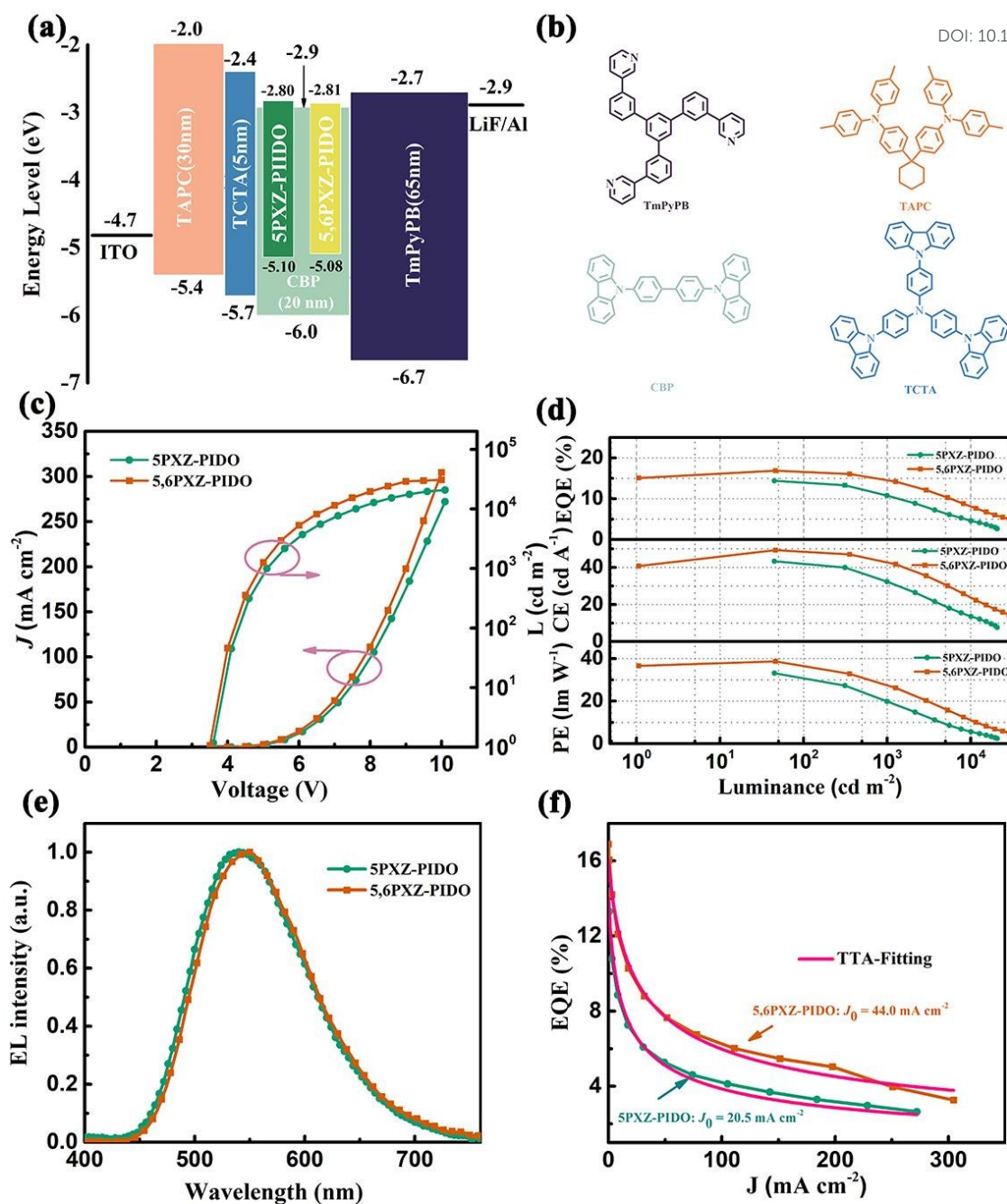


**Fig. 5** (a) The energy level diagrams and (b) chemical structures of the materials used for the devices. (c) Current density-voltage-luminance curves of the devices. Inset: Electroluminescence spectra of devices A and B at a driving voltage of 10 V. (d) Power efficiency (PE), current efficiency (CE) and external quantum efficiency (EQE) versus luminance curves of the devices A-B. (e) Electroluminescence spectra of devices A and B at a driving voltage of 10 V. (f) The external quantum efficiency (EQE) as a function of current density and the fitting results according to the triplet-triplet annihilation (TTA, pink lines) mechanism.

**Table 2** Electroluminescence characteristics of the devices A and B.

Device	Emitter	Maximum Efficiency <sup>a</sup>	Luminance at 1000 cd m <sup>-2</sup>	Luminance at 10000 cd m <sup>-2</sup>	EQE roll-offs <sup>b</sup>	CIE <sup>c</sup> (x, y)
		CE, PE, EQE	CE, PE, EQE	CE, PE, EQE		
A	5PXZ-PIDO	43.3, 33.1, 14.4	32.3, 19.9, 10.8	13.5, 5.6, 4.6	25.0, 68.1	(0.39, 0.54)
B	5,6PXZ-PIDO	49.3, 38.7, 16.9	41.7, 26.2, 14.2	23.6, 10.8, 8.1	16.0, 52.1	(0.42, 0.53)

<sup>a</sup>The maximum efficiencies of CE (cd A<sup>-1</sup>), PE (lm W<sup>-1</sup>) and EQE (%). <sup>b</sup>The EQE roll-offs (%) at 1000 cd m<sup>-2</sup> and 10000 cd m<sup>-2</sup>. <sup>c</sup>The Commission Internationale de l'Eclairage coordinates recorded at 8 V.

maximum current efficiency ( $CE_{\max}$ ) of 43.3 cd A<sup>-1</sup>, a maximum power efficiency ( $PE_{\max}$ ) of 33.1 lm W<sup>-1</sup> and a maximum external quantum efficiency ( $EQE_{\max}$ ) of 14.4%. Comparatively, the higher  $\Phi_{\text{PL}}$  as well as larger  $k_{\text{RISC}}$  of 5,6PXZ-PIDO endowed device B with a better device performance of 49.3 cd A<sup>-1</sup>, 38.7 lm W<sup>-1</sup>, and 16.9% (Table 2). The charge-transporting balance could be another important factor for different device performance for devices A and B. To figure out this point, the hole-only device having the structure of ITO/TAPC (25 nm)/TCTA (5 nm)/CBP: 1.5 wt.% dopant (50 nm)/TCTA (5 nm)/TAPC (25 nm)/Al (100 nm) and electron-only device having the structure of ITO/TmPyPB (30 nm)/CBP: 1.5 wt.% dopant (50 nm)/TmPyPB (30 nm)/LiF (1 nm)/Al (100 nm) were fabricated. As shown in Fig. S14, both devices exhibited dominant hole-transporting ability and poor electron-transporting ability. This suggests that both devices possessed unbalanced charge-transporting ability. In this sense, the charge-transporting balance may not be the decisive factor for the better EL performance of 5,6PXZ-PIDO than 5PXZ-PIDO. Remarkably, the TADF feature of both emitters imparted both devices with over 10% EQEs, which are significantly higher than the theoretical limit of 5-10% for the conventional fluorescent OLEDs. These results clearly establish effective utilization of triplet excitons through TADF process. To determine how many excitons are utilized, exciton utilization efficiencies ( $\eta_{\text{eueS}}$ ) were estimated on the basis of the following equation:<sup>40</sup>

$$\eta_{\text{ext}} = \eta_{\text{eue}} \gamma \Phi_{\text{PL}} \eta_{\text{out}}$$

where  $\gamma$  is the charge balance factor,  $\eta_{\text{out}}$  stands for the out-coupling efficiency (EQE), considered as a constant of 0.2-0.3 for ITO glass substrate,  $\Phi_{\text{PL}}$  refers to the intrinsic  $\Phi_{\text{PL}}$  of the emissive layer. Given the perfect charge balance ( $\gamma = 1$ ) and relatively high  $\eta_{\text{out}}$  of 0.25 in the devices,  $\eta_{\text{eueS}}$  of both devices were estimated to be 80% and 88.9% for 5PXZ-PIDO and 5,6PXZ-PIDO, respectively.

To determine the possible energy loss in our devices, we have estimated the theoretical maximum  $\eta_{\text{ext}}$  for both devices using the following equation:<sup>38</sup>

$$\eta_{\text{ext}} = \gamma \eta_{\text{out}} \left\{ 0.25 \Phi_p + [0.75 + 0.25(1 - \Phi_p)] * \frac{\Phi_d}{1 - \Phi_p} \right\}$$

Considering the perfect charge balance ( $\gamma = 1$ ) and relatively high  $\eta_{\text{out}}$  of 0.2-0.3 in the devices, the theoretical maximum  $\eta_{\text{extS}}$  were estimated to be 10.5%-15.7% for the 5PXZ-PIDO-based device and 12.0%-18.9% for the 5,6PXZ-PIDO-based device. Consequently, the experimental maximum EQEs of both devices (14.4% for the 5PXZ-PIDO-based device and 16.9% for the 5,6PXZ-PIDO-based device) are very close to their theoretical values. These results suggest that both devices exhibited small energy loss.

Inspiringly, the short DF lifetimes of both emitters endow both devices with slow efficiency roll-off at high luminance (Table 2). Device A achieved a high EQE of 10.8% and a slow EQE roll-off of 25.0% at a high luminance of 1000 cd m<sup>-2</sup>. Comparatively, the shorter DF lifetime of 5,6PXZ-PIDO imparted device B with an ultra-slow efficiency roll-off character: at a practical luminance of 1000 cd m<sup>-2</sup>, the EQE slightly dropped to 14.2% with an ultra-slow EQE roll-off value of 16.0%; even at an extremely high luminance of 10000 cd m<sup>-2</sup>, the EQE remained as high as 8.1%. The superior performance

combination of high efficiency and ultra-slow efficiency roll-off for 5,6PXZ-PIDO-based device B is prominent among previously reported carbonyl-based TADF emitters (Table S5).<sup>20,30-32,34,35,41</sup> Generally, triplet-exciton-involved quenching processes, such as triplet-triplet annihilation (TTA), singlet-triplet annihilation (STA) and triplet-polaron quenching (TPQ), are the main reasons for efficiency roll-off at high luminance.<sup>42-45</sup> As shown in Fig. 6, TTA simulation matched well with the  $EQE-J$  curves for devices A and B, which suggests that TTA mechanism mainly accounts for efficiency roll-off of both devices. The equation for the TTA fitting is expressed as follows:<sup>19</sup>

$$\frac{\eta}{\eta_0} = \frac{J_0}{4J} \left( \sqrt{1 + 8 \frac{J}{J_0}} - 1 \right)$$

where  $\eta$  represents the EQE of the device,  $\eta_0$  refers to the initial EQE in the absence of TTA,  $J$  stands for the current density of the device, and  $J_0$  is the "onset" current density at  $\eta = \eta_0/2$ . When assuming the perfect charge balance in our devices, the  $J_0$  of device B based on 5,6PXZ-PIDO was estimated to be 44.0 mA cm<sup>-2</sup>, which is over two times as high as that of device A based on 5PXZ-PIDO (20.5 mA cm<sup>-2</sup>). We also fitted the  $EQE-J$  curves of both devices with the TPQ model. As shown in Fig. S16, the TPQ model did not fit well with the experimental curves for both devices. Furthermore, the TTA fitting lines deviated from the experimental  $EQE-J$  curves at high current density. This suggests that the STA mechanism may become dominant with the increased current density, which is consistent with the previous reports on excitons quenching processes in TADF OLEDs.<sup>43-46</sup> These results manifest that the short DF lifetime and large  $k_{\text{RISC}}$  of 5,6PXZ-PIDO alleviate TTA process in the EL process, and thereby suppress efficiency roll-off. Despite of their good device performance, the luminescence of both devices lasted only ca. 1 hour without encapsulation. This could be more associated with instability of the CBP host and the charge-transporting materials of TAPC and TmPyPB.<sup>47</sup> Maybe the lifetime of our devices would be improved by using suitable host and charge-transporting materials in the further study.

## Conclusion

In summary, we have designed and synthesized two TADF emitters by an appropriate combination of an IDO core with PXZ units *via* the phenylene  $\pi$ -bridges. Both emitters exhibited excellent thermal stability, suitable HOMO/LUMO levels, relatively high  $\Phi_{\text{PL}}$  and distinct TADF feature with short DF lifetimes. As a result, the 5,6PXZ-PIDO-based device exhibited intense yellow emission with a high EQE of 14.2% and an ultra-slow efficiency roll-off of 16.0% at the practical luminance of 1000 cd m<sup>-2</sup>. This work demonstrates the great potential of indandione-cored compounds as TADF emitters in OLEDs.

## Acknowledgements

We acknowledge financial support from the National Natural Science Foundation of China (51573141 and 91433201), the National Key R&D Program of China (2016YFB0401002), the National Basic Research Program of China (2015CB655002), Shenzhen Peacock Plan (KQTD20170330110107046) and the Natural Science Foundation for Distinguished Young Scholars of Hubei Province (2017CFA033).

## Conflicts of interest

There are no conflicts to declare.

## References

- 1 A. Endo, M. Ogasawara, A. Takahashi, D. Yokoyama, Y. Kato and C. Adachi, *Adv. Mater.*, 2009, **21**, 4802.
- 2 H. Uoyama, K. Goushi, K. Shizu, H. Nomura and C. Adachi, *Nature*, 2012, **492**, 234.
- 3 Q. Wei, P. Kleine, Y. Karpov, X. P. Qiu, H. Komber, K. Sahre, A. Kiriy, R. Lygaitis, S. Lenk, S. Reineke and B. Voit, *Adv. Funct. Mater.*, 2017, **27**, 1605051.
- 4 F. B. Dias, J. Santos, D. R. Graves, P. Data, R. S. Nobuyasu, M. A. Fox, A. S. Batsanov, T. Palmeira, M. N. Berberan-Santos, M. R. Bryce and A. P. Monkman, *Adv. Sci.*, 2016, **3**, 1600080.
- 5 H. Tsujimoto, D. G. Ha, G. Markopoulos, H. S. Chae, M. A. Baldo and T. M. Swager, *J. Am. Chem. Soc.*, 2017, **139**, 4894.
- 6 S. Feuillastre, M. Pauton, L. Gao, A. Desmarchelier, A. J. Riives, D. Prim, D. Tondelier, B. Geffroy, G. Muller, G. Clavier and G. Pieters, *J. Am. Chem. Soc.*, 2016, **138**, 3990.
- 7 K. Wu, T. Zhang, L. Zhan, C. Zhong, S. Gong, N. Jiang, Z. H. Lu and C. Yang, *Chem. – Eur. J.*, 2016, **22**, 10860.
- 8 P. Rajamalli, N. Senthilkumar, P. Gandeepan, P.-Y. Huang, M.-J. Huang, C.-Z. Ren-Wu, C.-Y. Yang, M.-J. Chiu, L.-K. Chu, H.-W. Lin and C.-H. Cheng, *J. Am. Chem. Soc.*, 2016, **138**, 628.
- 9 K.-C. Pan, S.-W. Li, Y. Y. Ho, Y. J. Shiu, W. L. Tsai, M. Jiao, W. K. Lee, C.-C. Wu, C.-L. Chung, T. Chatterjee, Y. S. Li, K.-T. Wong, H.-C. Hu, C.-C. Chen and M. T. Lee, *Adv. Funct. Mater.*, 2016, **26**, 7560.
- 10 Y. C. Li, X. L. Li, D. J. Chen, X. Y. Cai, G. Z. Xie, Z. Z. He, Y. C. Wu, A. Lien, Y. Cao and S.-J. Su, *Adv. Funct. Mater.*, 2016, **26**, 6904.
- 11 D.-Y. Chen, W. Liu, C.-J. Zheng, K. Wang, F. Li, S. L. Tao, X.-M. Ou and X.-H. Zhang, *ACS Appl. Mater. Interfaces.*, 2016, **8**, 16791.
- 12 K. Suzuki, S. Kubo, K. Shizu, T. Fukushima, A. Wakamiya, Y. Murata, C. Adachi and H. Kaji, *Angew. Chem., Int. Ed.*, 2015, **127**, 15446.
- 13 D. R. Lee, M. Kim, S. K. Jeon, S.-H. Hwang, C. W. Lee and J. Y. Lee, *Adv. Mater.*, 2015, **27**, 5861.
- 14 Y. Kitamoto, T. Namikawa, D. Ikemizu, Y. Miyata, T. Suzuki, H. Kita, T. Sato and S. Oi, *J. Mater. Chem. C*, 2015, **3**, 9122.
- 15 H. Kaji, H. Suzuki, T. Fukushima, K. Shizu, K. Suzuki, S. Kubo, T. Komino, H. Oiwa, F. Suzuki, A. Wakamiya, Y. Murata and C. Adachi, *Nat. Commun.*, 2015, **6**, 8476.
- 16 H. Wang, L. Xie, Q. Peng, L. Meng, Y. Wang, Y. Yi and P. Wang, *Adv. Mater.*, 2014, **26**, 5198.
- 17 W. Zeng, H.-Y. Lai, W.-K. Lee, M. Jiao, Y.-J. Shiu, C. Zhong, S. Gong, T. Zhou, G. Xie, M. Sarma, K.-T. Wong, C.-C. Wu and C. Yang, *Adv. Mater.*, 2018, **30**, 1704961.
- 18 T.-A. Lin, T. Chatterjee, W. L. Tsai, W.-K. Lee, M. J. Wu, M. Jiao, K.-C. Pan, C. L. Yi, C.-L. Chung, K.-T. Wong and C.-C. Wu, *Adv. Mater.*, 2016, **28**, 6976.
- 19 Y. P. Xiang, Y. B. Zhao, N. Xu, S. L. Gong, F. Ni, K. L. Wu, J. J. Luo, G. H. Xie, Z. H. Lu and C. L. Yang, *J. Mater. Chem. C*, 2017, **5**, 12204.
- 20 X. Cai, D. Chen, K. Gao, L. Gan, Q. Yin, Z. Qiao, Z. Chen, X. Jiang and S.-J. Su, *Adv. Funct. Mater.*, 2018, **28**, 1704927.
- 21 T.-L. Wu, M.-J. Huang, C.-C. Lin, P.-Y. Huang, T.-Y. Chou, R.-W. Chen-Cheng, H.-W. Lin, R.-S. Liu and C.-H. Cheng, *Nat. Photon.*, 2018, **12**, 235.
- 22 P. K. Samanta, D. Kim, V. Coropceanu and J.-L. Brédas, *J. Am. Chem. Soc.*, 2017, **139**, 4042.
- 23 M. K. Etherington, J. Gibson, H. F. Higginbotham, T. J. Penfold and A. P. Monkman, *Nat. Commun.*, 2016, **7**, 13680.
- 24 C. Duan, J. Li, C. Han, D. Ding, H. Yang, Y. Wei and H. Xu, *Chem. Mater.*, 2016, **28**, 5667.
- 25 D. Deng, Y. Zhang, J. Zhang, Z. Wang, L. Zhu, J. Fang, B. Xia, Z. Wang, K. Lu, W. Ma and Z. Wei, *Nat. Commun.*, 2016, **7**, 13740.
- 26 M. Li, S.-H. Li, D. Zhang, M. Cai, L. Duan, M.-K. Fung and C.-F. Chen, *Angew. Chem., Int. Ed.*, 2018, **57**, 2889.
- 27 A. Steingeger, I. Klimant and S. M. Borisov, *Adv. Opt. Mater.*, 2017, **5**, 1700372.
- 28 J. Hou, O. Inganäs, R. H. Friend and F. Gao, *Nat. Mater.*, 2018, **17**, 119.
- 29 P. Rajamalli, N. Senthilkumar, P. Y. Huang, C. C. Ren-Wu, H. W. Lin and C. H. Cheng, *J. Am. Chem. Soc.*, 2017, **139**, 10948.
- 30 S. Y. Lee, T. Yasuda, Y. S. Yang, Q. Zhang and C. Adachi, *Angew. Chem., Int. Ed.*, 2014, **53**, 6402.
- 31 J. Huang, H. Nie, J. Zeng, Z. Zhuang, S. Gan, Y. Cai, J. Guo, S. J. Su, Z. Zhao and B. Z. Tang, *Angew. Chem., Int. Ed.*, 2017, **56**, 12971.
- 32 S. Y. Lee, T. Yasuda, I. S. Park and C. Adachi, *Dalton. Trans.*, 2015, **44**, 8356.
- 33 J.-X. Chen, W. Liu, C.-J. Zheng, K. Wang, K. Liang, Y.-Z. Shi, X.-M. Ou and X.-H. Zhang, *ACS Appl. Mater. Interfaces.*, 2017, **9**, 8848.
- 34 K. Nasu, T. Nakagawa, H. Nomura, C.-J. Lin, C.-H. Cheng, M.-R. Tseng, T. Yasuda and C. Adachi, *Chem. Commun.*, 2013, **49**, 10385.
- 35 J. Guo, X. L. Li, H. Nie, W. Luo, S. Gan, S. Hu, R. Hu, A. Qin, Z. Zhao, S. J. Su and B. Z. Tang, *Adv. Funct. Mater.*, 2017, **27**, 1606458.
- 36 J. P. N. Papillon, C. M. Adams, Q.-Y. Hu, C. Lou, A. K. Singh, C. Zhang, J. Carvalho, S. Rajan, A. Amaral, M. E. Beil, F. Fu, E. Gangl, C.-W. Hu, A. Y. Jeng, D. LaSala, G. Liang, M. Logman, W. M. Maniara, D. F. Rigel, S. A. Smith and G. M. Ksander, *J. Med. Chem.*, 2015, **58**, 4749.
- 37 H. Tanaka, K. Shizu, H. Nakanotani and C. Adachi, *Chem. Mater.*, 2013, **25**, 3766.
- 38 Y. Xiang, S. Gong, Y. Zhao, X. Yin, J. Luo, K. Wu, Z.-H. Lu and C. Yang, *J. Mater. Chem. C*, 2016, **4**, 9998.
- 39 W. Yoshimasa, K. Shosei and K. Hironori, *Adv. Mater.*, 2018, **30**, 1705641.
- 40 J. Luo, G. Xie, S. Gong, T. Chen and C. Yang, *Chem. Commun.*, 2016, **52**, 2292.
- 41 Q. Zhang, H. Kuwabara, W. J. Potscavage, S. Huang, Y. Hatae, T. Shibata and C. Adachi, *J. Am. Chem. Soc.*, 2014, **136**, 18070.
- 42 J. Ye, C.-J. Zheng, X.-M. Ou, X.-H. Zhang, M.-K. Fung, C.-S. Lee, *Adv. Mater.*, 2012, **24**, 3410.
- 43 M. A. Baldo, C. Adachi and S. R. Forrest, *Phys. Rev. B.*, 2000, **62**, 10967.
- 44 C. Murawski, K. Leo and M. C. Gather, *Adv. Mater.*, 2013, **25**, 6801.
- 45 K. Masui, H. Nakanotani and C. Adachi, *Org. Electron.*, 2013, **14**, 2721.
- 46 Z. Wang, Y. Li, X. Cai, D. Chen, G. Xie, K. Liu, Y.-C. Wu, C.-C. Lo, A. Lien, Y. Cao and S.-J. Su, *ACS Appl. Mater. Interfaces.*, 2016, **8**, 8627.

## ARTICLE

Journal Name

47 L. Zhang, Y.-X. Zhang, Y. Hu, X.-B. Shi, Z.-Q. Jiang, Z.-K. Wang  
and L.-S. Liao, *ACS Appl. Mater. Interfaces*, 2016, **8**, 16186.

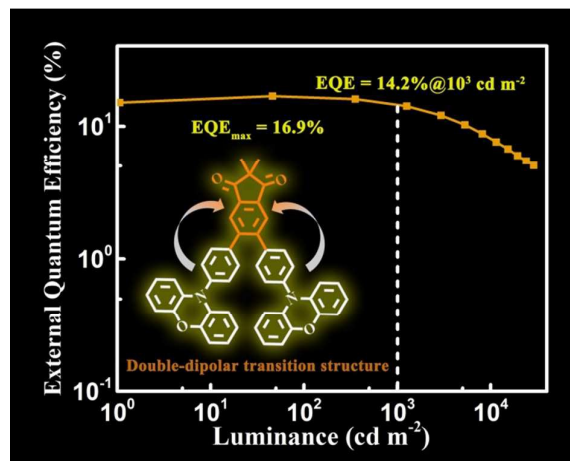
48

View Article Online  
DOI: 10.1039/C8TC01656A

Journal of Materials Chemistry C Accepted Manuscript

Published on 16 June 2018. Downloaded by University of Reading on 6/16/2018 4:29:34 PM.

## Table of contents



Two indandione-based compounds are demonstrated as yellow TADF emitters with short emissive lifetimes to simultaneously afford a high efficiency and a slow efficiency roll-off at the practical luminance levels.